Carbon Dioxide as a Working Fluid in Aircraft Air–Conditioning: an Experimental Assessment

ALBERTO CAVALLINI, *Full Professor, University of Padova, Italy.* alcav@unipd.it
ACHILLE MANNINI, *Microtecnica s.r.l., Italy.* achille.mannini@hs.utc.com
PIETRO ASINARI, *Research Scientist, Politecnico di Torino, Italy.* pietro.asinari@polito.it
CLAUDIO ZILIO, *Assistant Professor, University of Padova, Italy.* claudio.zilio@unipd.it

ABSTRACT

The design of an experimental test rig for characterizing the thermal performances of a refrigerating device based on a carbon dioxide transcritical cycle for airborne application is discussed. This experimental test rig proves that the transcritical device can properly match the required specifications in order to be integrated with a conventional air–cycle machine and to realize in this way a hybrid air conditioning system for airborne application. Some practical solutions for managing the integration between the conventional system and the vapor cycle system are discussed on the basis of the experimental results.

1. INTRODUCTION

1.1 Traditional Environmental Control System for airborne air-conditioning

In the aircraft industry, the term Environmental Control System (ECS) is used to identify the devices realizing suitable environmental conditions for passengers and crew inside the cabin. ECS includes systems and equipment associated with the ventilation, heating, cooling, humidity/contamination control and pressurization in the passenger and cargo compartments, and the electronic equipment bays (ASHRAE 1998, Hunt *et al.* 1995). Environmental control systems of various type and complexity are used in military and civil aircraft, helicopter and spacecraft applications. In the following, only commercial transport aircraft will be considered. For this market application, air–cycle air conditioning for the ECS represents the largely predominant strategy. The Brayton refrigeration cycle is generally preferred to the Evans–Perkins cycle. This strategy is usually a matter of convenience due to the easiness of extracting compressed air from engine bleeds but it enormously increases the energy consumption for air–conditioning.

Aircraft ECSs operate under very extreme conditions because the external physical environment during flight conditions is not survivable by unprotected humans. Outside air at cruise altitude is extremely cold, dry and can contain high levels of ozone. On the other hand, while on the ground air can be hot, humid, and contain many pollutants, such as particulate matter, aerosols and hydrocarbons. These ambient conditions change quickly from ground operations to flight. In addition to essential safety requirements, the ECS should provide a comfortable environment for the passengers and the crew. This is complicated by the high seating density of the passengers, the changes in cabin pressure and the changes of outside environment during flight.

The core of conventional ECSs is realized by the Air Cycle System (ACS). The ACS realizes the requested cooling capacity by means of a Brayton inverse cycle. Essentially this process can be realized in three steps. Ambient air compressed by the engine compressor provides the power input, the heat of compression is removed in a heat exchanger using ambient air as heat sink and finally the cooled air is refrigerated by expansion across a turbine. The turbine energy resulting from expansion is absorbed by an auxiliary machine, which is either a ram air fan, a further bleed air compressor or both (ASHRAE, 1998). Moisture condensed during the refrigeration process is removed by a water separator. The most common types of air–conditioning cycles in use on commercial transport aircraft are: the two–wheel bootstrap ACS consisting of a turbine and an auxiliary compressor which further compresses the bleeded air; the three–wheel ACS consisting of a turbine, an auxiliary compressor and a fan which moves the ambient air needed for cooling the compressed air before expansion and, finally, the four–wheel ACS consisting of two turbines which allow intermediate removal of the moisture, an auxiliary compressor and a fan. The three–wheel ACS is used on most of the newer commercial aircrafts, including commuter aircrafts and business aircrafts. The four–wheel ACS was first applied on the Boeing 777 aircraft and it is still used today.

1.2 New challenges for reducing energy consumption of Environmental Control System

The traditional picture of the ECS is nowadays under discussion. In fact the goal of reducing energy consumption due to transportation is considered a top priority issue and it will effect the aircraft industries in the next years by forcing the development of new technological solutions. Many research and development programs have been founded in order to reach this goal. For example, the Power Optimised Aircraft project (POA 2002–2005) is the most recent and most integrated project to address the creation of a more efficient aircraft. At the aircraft level, the project should demonstrate a 25 % reduction in peak non–propulsive power usage, a 5 % reduction in fuel consumption, a reduction in equipment weight and no degradation in production costs, maintenance costs or reliability.

According to other mobile applications, for example automotive and marine applications, some evidence exists about the fact that a more widespread electrical power distribution would allow us to consider more efficient components and a more flexible management of the energy demand. Both these advantages can yield an increase in the whole efficiency. This optimized solution at total aircraft level is certain to define an improvement that any solution at systems level can no longer provide (Faleiro 2004).

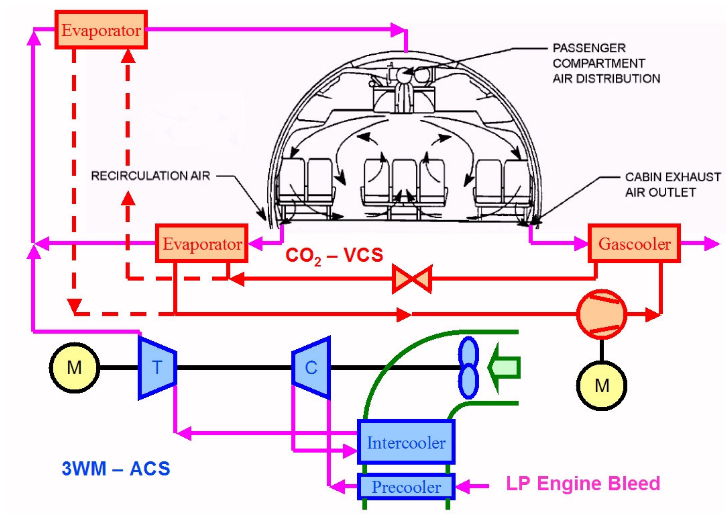

Figure 1 – Hybrid ECS based on a three-wheel motorized ACS (3WM-ACS) and a carbon dioxide VCS.
The motor involved in the air cycle allows us to consider low pressure (LP) engine bleed
for the air supply. Two positions of the evaporator in the ECS architecture are considered.

Improving electrical power distribution and increasing the number of the electrical systems can also open some new opportunities for the ECS. In particular, compressors driven by electrical motors can be used in a more efficient Vapor Compression System (VCS), i.e. a system based on a proper closed refrigerant circuit which realizes an Evans–Perkins cycle. In this way, during the whole aircraft mission profile except descent, the ACS is capable to satisfy pressurization and ventilation and the VCS (configured eventually as heat pump) could support the ACS for cooling/heating. This system could be defined a hybrid ECS because it is composed of two subsystems which realize different thermodynamic reference cycles. Two possible integration strategies between subsystems are reported in Fig. 1. The refrigerant cooler can be conveniently installed at the cabin exhaust air outlet. Even though the comfort temperature inside the cabin does not ensure the lowest heat sink for the refrigerant cooler (during flight condition the external temperature is usually much lower), this solution allows us to avoid any additional external air inlet and ensure stable operating conditions. The evaporator can be installed in, at least, two promising locations:

a) after the mixing point (AM) between recirculated air taken from the cabin and the refrigerated air, as in the three–wheel ACS (see dashed lines in Fig. 1);
b) before the mixing point (BM) in the recirculation air duct which takes air from the cabin (see continuous lines in Fig. 1).

In the first configuration (AM), the evaporator would receive a great air mass flow rate, which is the sum of recirculation and ACS mass flow rate, but it would work with quite low air inlet temperature because of the ACS cooling capacity. The great air mass flow rate tends to reduce the thermal resistance at the evaporator with consequent positive effects in terms of efficiency, while the low air inlet temperature requires low evaporating temperature for the refrigerant and this usually penalizes the compressor. On the other hand, in the second configuration (BM), the situation is reversed because the evaporator would receive a moderate air mass flow rate equal to the fresh flow requirement, but it would work with a higher air inlet temperature equal to the cabin comfort temperature. On the basis of the previous considerations, it is not clear what of these configurations is the best in terms of energy saving. The comparison depends on operating conditions, working fluid, system architecture and adopted components.

Concerning the working fluids, the natural fluids should be considered in order to avoid any future regulation constraint, as it happens now with the air cycle machines. Among the natural fluids for refrigeration, carbon dioxide seems suitable for this application. First of all high working pressures in refrigerant cycles based on carbon dioxide imply a reduction of the refrigerant charge and consequently more compact compressors and lighter machines. Secondly the thermophysical properties of carbon dioxide are favorable to produce high heat transfer coefficients in the heat exchangers of the equipment (of suitable geometry), often higher than those commonly obtained with traditional synthetic refrigerants. Finally carbon dioxide is a product that displays no special local safety problem, as it is non–flammable and non–toxic.

In order to understand what constraints limit the design process and what configuration yields the best performance for the transcritical refrigerating cycles based on carbon dioxide, an experimental test rig has been developed, particularly dealing with the airborne application.

2. DESIGN AND CONSTRUCTION OF THE EXPERIMENTAL TEST RIG

2.1 Goals and general framework

An experimental test rig, which reproduces as close as possible the operating conditions of a vapor compression subsystem integrated in a hybrid ECS, has been built by Microtecnica s.r.l. in the framework of the on–going effort for substituting conventional air–based ECS in commercial aircrafts.

The main goals of this activity are:

a) to produce a coherent set of measurements which will be used to calibrate a simplified mathematical model needed to characterize the vapor compression subsystem (Vankan *et al.* 2003);
b) to supply some experimental evidences which allow us to select the most suitable integration strategy between the vapor cycle and the air cycle subsystem, needed to define the whole hybrid ECS (the two most promising strategies are reported in Fig. 1).

The selected experiments must be as close as possible to the actual operating conditions of the installed VCS. Unfortunately, a full capacity test rig would be too expensive at this stage because of the lack of existing components for aircraft application. For this reason, smaller components, derived from automotive application, were considered in this work and a proper scaling strategy was also considered.

The steady–state cooling load for a particular aircraft model can be calculated by a heat transfer study of several elements (convection at outer aircraft skin, radiation from external environment, solar radiation through glasses, conduction through aircraft structure, convection at interior aircraft skin,...). These calculations allow us to estimate the refrigerating thermal power needed by the particular aircraft model. Usually, this cooling request is split between two identical ECSs in order to guarantee at least half of the cooling capacity, in case of single system failure. In the present application, this ideal process is more complicate by the fact that the cooling capacity must be further split between the VCS and the ACS which make the ECS.

The experimental test rig aims to generate one third of the full cooling capacity for both ground and flight conditions. In order to realize similar temperature profiles and to reproduce operating conditions as close as possible to those of the actual machine at aircraft level, the air mass flow rates for both heat exchangers were chosen to be one third of the actual values too. The heat exchanger inlet temperatures were increased in order to take into account local heatings due to fans and auxiliary devices.

2.2 Test rig components and architecture selection

In the design of the VCS experimental test rig, existing prototype components have been taken from automotive application because it shares the same need for lightweight and ultra–compact components. Practically the simplified design of the experimental test rig required to find the best architecture satisfying the desired performance and reducing the number of components to the minimum value.

Table 1. Numerical simulations for different system architectures: simple *architecture A* with one–slab gascooler and one–slab evaporator; improved *architecture B* with two–slab gascooler, one–slab evaporator and internal heat exchanger; best *architecture C* with two–slab gascooler, two–slab evaporator and internal heat exchanger.

Architecture	A	B	C
Coefficient of performance $[-]$	0.840	1.434	1.543
Refrigerant mass flow rate $[kg/s]$	0.088	0.056	0.061
Cooling capacity $[kW]$	3.812	6.426	6.970
Mechanical compression power $[kW]$	4.538	4.483	4.517
Rejected thermal power $[kW]$	7.149	10.224	10.526
Wasted compressor thermal power $[kW]$	0.482	0.642	0.643
Wasted discharge line thermal power $[kW]$	0.689	0.371	0.404
Internal thermal power $[kW]$	-	3.289	3.890
Evaporator			
Cooled air mass flow rate $[kg/s]$	0.334	0.334	0.334
Inlet cooled air temperature $[℃]$	25.0	25.0	25.0
Inlet cooled air humidity ratio $[g/kg]$	1.950	1.950	1.950
Outlet cooled air temperature $[℃]$	13.7	6.8	5.0
Outlet cooled air humidity ratio $[g/kg]$	1.947	1.949	1.947
Gascooler			
Cooling air mass flow rate $[kg/s]$	0.326	0.326	0.326
Inlet cooling air temperature $[℃]$	30.0	30.0	30.0
Outlet cooling air temperature $[℃]$	51.3	60.5	61.4

Since the required cooling capacity for the present test rig is greater than that of a conventional air conditioning system for automotive applications, multi–slab configurations for heat exchangers is needed. In order to evaluate the proper architecture for the present application, some numerical simulations were run (see Tab. 1). A numerical code previously developed was used for this purpose (Cecchinato *et al.* 2003) and small changes were introduced (internal heat exchanger) in order to describe the architectures under investigation. The numerical code requires detailed geometrical and topological data of both heat exchangers in order to match real devices and some compressor global performance data.

The numerical results show that, in order to match the required cooling capacity, the gascooler heat transfer surface must be increased for reducing the approach temperature and consequently reducing the gascooler outlet enthalpy, which is equal to the evaporator inlet enthalpy. Moreover an internal heat exchanger must be included in the test rig layout for realizing an evaporation process completely in the two–phase region (vapor mass fraction is in the range 0.4÷0.9).

Once the heat transfer surfaces have been defined, it is possible to select the proper compressor and the proper rotational speed, which realizes the desired refrigerant mass flow rate. The selected compressor derives from a mobile application too (bus air conditioning). Taking into account the swept volume, some very easy calculations allow us to estimate the rotational speed required by *architecture C* (see Tab. 1).

In transcritical refrigerating cycles, the high–pressure side is no more related to the temperature field inside the heat exchanger designed for heat rejection. For this reason, the high–pressure side becomes a tunable parameter which must be controlled in order to ensure the best COP (Cavallini 1996). In the present application, an automatic throttling valve with position feedback control and a low–pressure receiver as refrigerant buffer at evaporator outlet have been adopted.

In addition to the refrigerant circuit, the experimental test rig is made by two air circuits which simulate the thermal load (evaporator air circuit) and the heat rejection sink (gascooler air circuit) as close as possible to actual operating conditions at aircraft level. The evaporator is housed in a closed air circuit, while the gascooler is housed in an open air circuit which can take air from the external environment or partially recirculate it in order to reduce the energy consumption. Both the air circuits involve an air fan which generates the desired mass flow rate, a calibrated orifice for measurement purposes and a local heater. The local heater of the evaporator air circuit must compensate the cooling capacity realized by the refrigerating circuit.

The experimental test rig was equipped with some transducers which allowed us to perform the measurements and to collect the feedback signals for the controlled devices. Essentially the network of transducers has been designed in order to completely characterize the actual thermodynamic cycle and to estimate the air–side thermal powers involved in both air circuits. The last feature enables to check the thermal balance of each heat exchanger and to consequently verify the reliability of the experimental results.

A refrigerant–side schematic of the experimental test rig is reported in Fig. 2, while a global picture showing the whole test rig is reported in Fig. 3.

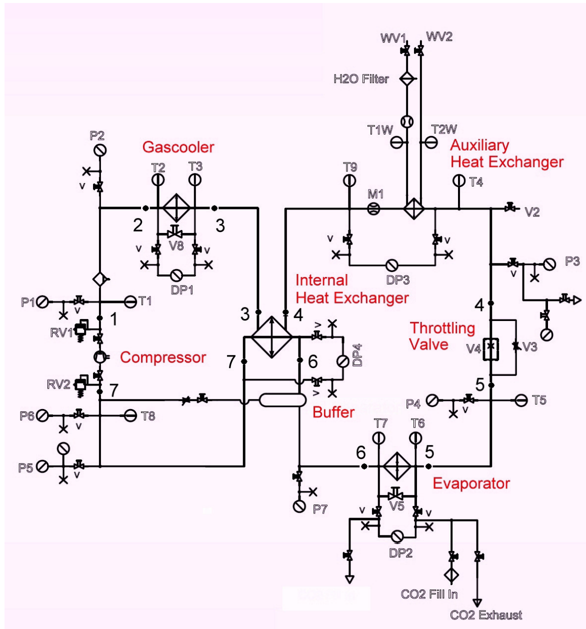

Figure 2 – Refrigerant-side schematic of the experimental test rig (courtesy of Microtecnica s.r.l.).

Figure 3 – Vapor Cycle Subsystem test rig (courtesy of Microtecnica s.r.l.).

3. EXPERIMENTAL RESULTS

3.1 Design of experiments and reliability checking

The design of experiments deals with the problem of deciding what pattern of experimental test conditions will best reveal aspects of investigated phenomena (Box *et al.* 1978). To perform a general experimental design, a fixed number of discrete values ("levels") for each of a number of variables ("factors") is selected and then all the possible combinations are experimentally considered. The goal of the experimental design is to characterize how the investigated quantity ("response") depends on considered factors.

For the present application, there are six meaningful factors: the air mass flow rate at the evaporator inlet; the air mass flow rate at the gascooler inlet; the air temperature at the evaporator inlet; the air temperature at the gascooler inlet; the working pressure at the gascooler outlet and finally the refrigerant mass flow rate. Possible responses are the cooling capacity Φ_e, the rejected thermal power Φ_g and the thermal coefficient of performance $TCOP$. The $TCOP$ is defined as:

$$TCOP = \frac{\Phi_e}{\Phi_g + (\Phi_{rh} - \Phi_{rl}) + \Phi_d - \Phi_e} = \frac{\Phi_e}{W_c - \Phi_c} \quad (1)$$

where Φ_{rh} is the high–pressure–side thermal power due to the internal heat exchanger, Φ_{rl} is the low–pressure–side thermal power due to the internal heat exchanger, Φ_d is the thermal power waste of the compressor discharge line, W_c is the mechanical power absorbed by the compressor and Φ_c is the compressor thermal power waste. The $TCOP$ differs from the usual coefficient of performance $COP = \Phi_e / W_c$.

The refrigerant pressure at the gascooler outlet should be set equal to the optimal value for the considered approach temperature in order to realize the maximum COP. Moreover, the refrigerant mass flow rate and the volumetric efficiency are mainly a result of the compressor rotational speed because suction does not change too much for the considered operating conditions. For this reason, only the air–side quantities will be considered for the experimental design (4 factors). The minimum number of levels (2 levels: maximum and minimum value) will be considered for all factors. The previous assumptions define a $2^4 = 16$ factorial design.

Pressure, temperature and specific enthalpy for the cornerstones of the thermodynamic cycle were measured. It was not possible to repeat the experimental tests a number of times suitable for evaluating the statistical scattering due to experimental inaccuracies. For this reason, the previous data are not provided with their error bars, but at least the accuracy of the instrument was considered: this is ±0.7 bar for the pressure transducers, ±0.2 °C for the temperature transducers and finally ±0.6 kJ/kg for the indirect enthalpy estimation.

Table 2. Comparison between air–side (AS) and refrigerant–side (RS) measurements.

	Thermal Power							
	Gascooler $[kW]$			Evaporator $[kW]$			Internal	TCOP
	Air-Side	Refr.-Side	R	Air-Side	Refr.-Side	R	$[kW]$	$[-]$
1	10.88	10.45	3.97	8.31	7.27	12.50	3.83	1.93
2	10.69	10.46	2.15	8.11	7.13	12.00	3.85	1.82
3	11.83	11.39	3.75	9.41	8.02	14.78	3.34	2.04
4	11.52	11.28	2.12	8.99	7.78	13.40	3.42	1.91
5	10.83	10.43	3.73	8.19	7.09	13.34	3.65	1.81
6	10.57	10.35	2.06	7.82	6.91	11.65	3.75	1.71
7	11.59	11.25	2.94	9.10	7.78	14.51	3.38	1.92
8	11.31	11.15	1.39	8.78	7.58	13.73	3.51	1.81
9	11.87	11.16	6.04	7.20	6.74	6.81	6.06	1.33
10	11.77	11.31	3.91	7.06	6.71	5.19	6.16	1.27
11	12.89	12.32	4.44	8.38	7.71	8.69	5.83	1.46
12	12.77	12.40	2.92	8.01	7.58	5.69	6.03	1.38
13	11.80	11.41	3.33	7.17	6.73	6.56	6.22	1.26
14	11.57	11.32	2.16	6.85	6.59	3.81	6.29	1.21
15	12.65	12.31	2.73	8.12	7.54	7.64	5.90	1.39
16	12.54	12.38	1.21	7.90	7.44	6.21	5.99	1.32

Since both air circuits are provided with temperature transducers (the effects due to moisture content can be neglected), it is possible to verify the thermal balance for both main heat exchangers. The post–processed experimental results are reported in Tab. 2. The difference between air–side and refrigerant–side measurements with regard to transferred thermal power are very good for the gascooler. In this case, the relative error on the thermal balance is less than 6 %. Unfortunately the same error for the evaporator is much higher and it can be equal to 15 % as maximum value. This error is not due to the simplifying assumption of neglecting the latent thermal power. In fact this error means that the air–side estimation overestimates the transferred thermal power. Since only the sensible thermal power is measured, at most the air–side estimation should be smaller than refrigerant–side one, which involves both sensible and latent thermal power. Moreover the error is a monotonic increasing function of the air mass flow rate at the evaporator: the average error is around 6 % for 0.27 kg/s and 13 % for 0.33 kg/s. It is plausible to suppose that the error is mainly due to an air leakage in the evaporator air circuit between the measurement section for the air mass flow rate and the evaporator inlet. This means that a slightly reduced fraction of the measured air mass flow rate really passes through the evaporator and it is involved in the heat transfer process.

3.2 Data fitting and analysis

In order to analyze the experimental results a best–fitting technique has been used in order to produce a smooth set of data, consistent with the original discrete input data (Box *et al.* 1978). Hence the interpolated model was used for analyzing the effects due to the VCS installation strategy: evaporator installed after the mixing point (AM) between recirculated air taken from the cabin and the refrigerated air (see dashed lines in Fig. 1) or before the mixing point (BM) in the recirculation air duct which takes air from the cabin (see continuous lines in Fig. 1).

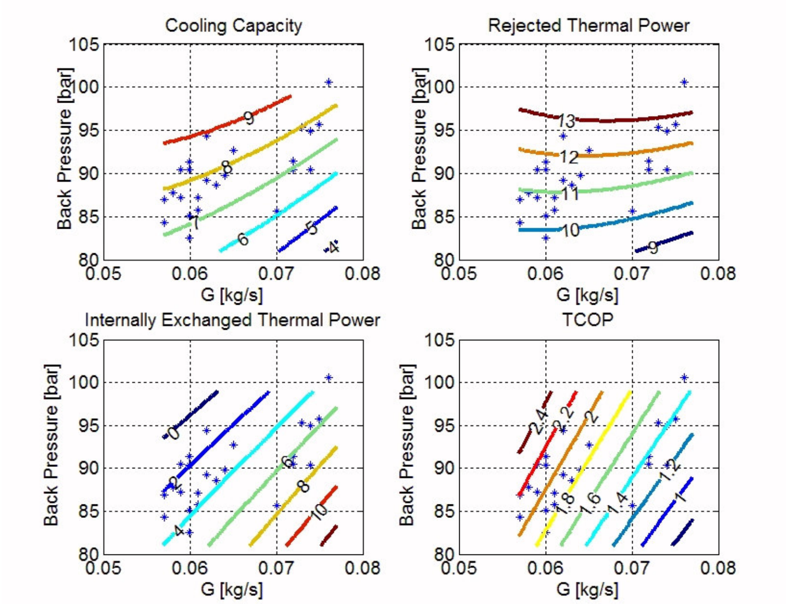

Figure 4 – Numerical results due to the interpolation model: effects of refrigerant mass flow rate and set point of back–pressure valve with evaporator installed after the mixing point (see Fig. 1).

Both previous configurations were investigated by calculating the cooling capacity, the rejected thermal power, the internal thermal power and the TCOP are reported. In particular in Fig. 4, the numerical results for the installation after the mixing point are reported The asterisks denote the actual experimental measurements. The air–side conditions for the gascooler are the same in both cases. The effects of the refrigerant mass flow rate and the set point of the back–pressure valve are also investigated. These previous results are substantially identical for both configurations. This seems somehow to prove the idea that the two configurations are equivalent, but they are not. In fact, the real systems do not work with a fixed refrigerant mass flow rate. In the electrified aircraft architecture, the compressor will be powered by an electrical motor controlled by an inverter and the feedback will be on the rotational speed. For this reason, the effective refrigerant mass flow rate can change according to the density of the actual suction condition. The same holds for the reported experimental design. Usually the suction density decreases when the air mass flow rate at the evaporator increases. In fact, high air mass flow rate at the evaporator enhances the efficiency of the evaporator and consequently also the super–heating. Working with a fixed rotational speed leads to a consequent reduction of the refrigerant mass flow rate. As shown in the bottom–right sub–plots of Fig. 4, reducing the refrigerant mass flow rate for a given set point of the back–pressure valve increases the TCOP. Moreover, as shown in the top–left sub–plots in the same figure, this slightly increases the cooling capacity too. For this reason, the after–mixing (AM) installation strategy (see Fig. 1) for the evaporator is preferable for reducing the energy consumption, and this can slightly increase the cooling capacity too. Actually the air mass flow rate at the evaporator does not directly affect the performances of the transcritical cycle but it reduces the suction density, consequently the refrigerant mass flow rate and this is enough to increase the whole performance.

4. CONCLUSIONS

In this paper, the design of an experimental test rig which enables us to characterize the thermal performances of a refrigerating device based on a carbon dioxide transcritical cycle have been discussed. The final goal of this experimental test rig is to prove that the transcritical device can properly match the required specifications in order to be integrated with a conventional air–cycle machine and to realize in this way a hybrid air conditioning system for airborne application. In particular, the experimental results show that the best installation strategy for integrating the vapor compression system with the air cycle system deals with installing the evaporator after the mixing point between recirculated air taken from the cabin and the refrigerated air.

5. ACKNOWLEDGEMENTS

This work was sponsored by Microtecnica s.r.l., a Hamilton Sundstrand company. Pietro Asinari would like to acknowledge Prof. Michele Calì for creating the conditions for the development of the present work.

NOMENCLATURE

COP	coefficient of performance
TCOP	thermal coefficient of performance
W	mechanical power
Φ	thermal power

Other subscripts:

c	compressor
d	discharge line
e	evaporator
g	gascooler
rh	regenerative high–pressure side
rl	regenerative low–pressure side

REFERENCES

ASHRAE, *ASHRAE Handbook: Applications*, Atlanta, GA: American Society of Heating, Refrigerating and Air–Conditioning Engineers (1998).

E. H. Hunt, D. H. Reid, D. R. Space, F. E. Tilton, Commercial airliner environmental control systems: engineering aspects of cabin air quality, *Proceedings of the Aerospace Medical Association Annual Meeting*, Anaheim (CA) (1995).

Power Optimised Aircraft, Contract Number G4RD-CT-2001-00601 under the European Community 5th Framework Programme for Research – Competitive Sustainable Growth – Key Action: *New Perspectives in Aeronautics*, www.poa-project.com (2002 – 2005).

L. F. Faleiro, Trends towards a more electrical aircraft, Liebherr–Aerospace, Lindenberg (DE), www.poa-project.com (2004).

W. J. Vankan, J. Kos, W. F. Lammen, Approximation models for multi-disciplinary system design - Application in a design study for power optimised aircraft, *Proceedings of the International Congress on Evolutionary Methods for Design, Optimization and Control with Applications to Industrial Problems EUROGEN 2003*, Barcelona, www.poa-project.com (2003).

L. Cecchinato, M. Corradi, E. Fornasieri, L. Zamboni, Carbon dioxide as refrigerant for tap water heat pumps: a comparison with the traditional solution, *Proceeding of XXI IIR International Congress of Refrigeration*, Washington D.C., USA (2003).

P. Asinari, Multi–Scale Analysis of Heat and Mass Transfer in Mini/Micro–Structures, *Ph.D. Dissertation*, Politecnico di Torino, 2005.

M.–H. Kim, J. Pettersen, C. W. Bullard, Fundamental process and system design issues in CO_2 vapor compression systems, *Progress in Energy and Combustion Science*, Vol. 30, pp. 119-174 (2004).

University of Padova, Use of natural working fluids in air conditioning, *Natural fluid vapour cycle Task 6.3, Confidential report with Power Optimized Aircraft POA* (2002).

A. Cavallini, Working fluids for mechanical refrigeration – invited paper presented at the 19th international congress of refrigeration, *International Journal of Refrigeration*, Vol. 19, No. 8, pp. 485-496 (1996).
G. E. P. Box, W.G. Hunter, J. S. Hunter, *Statistics for experimenters*, John Wiley & Sons, New York (1978).